Forschungszentrum Karlsruhe
Technik und Umwelt
Wissenschaftliche Berichte
FZKA 6580

The Multiwire Proportional Chambers in the Central Detector of KASCADE

H. Bozdog, M. Elzer, H. J. Gils, A. Haungs, F. Herm, H. Koepernik, K. U. Köhler, M. Kretschmer, H. Leibrock, H. J. Mathes, M. Petcu, D. Pröhl, H. Rebel, J. Wentz, A. Wolf, S. Zagromski

Institut für Kernphysik

Dezember 2000

Forschungszentrum Karlsruhe
Technik und Umwelt
Wissenschaftliche Berichte
FZKA 6580

The Multiwire Proportional Chambers in the Central Detector of KASCADE

H. Bozdog[a], M. Elzer, H.J. Gils, A. Haungs, F. Herm, H. Koepernik[b], K.U. Köhler, M. Kretschmer, H. Leibrock, H.J. Mathes, M. Petcu[a], D. Pröhl[b], H. Rebel, J. Wentz, A. Wolf[b], S. Zagromski

Institut für Kernphysik

[a] National Institute of Physics and Nuclear Engineering, Bucharest, Romania

[b] Forschungszentrum Rossendorf e.V., Dresden, Germany

Forschungszentrum Karlsruhe GmbH, Karlsruhe
2000

Als Manuskript gedruckt

Forschungszentrum Karlsruhe GmbH
Postfach 3640, 76021 Karlsruhe

Mitglied der Hermann von Helmholtz-Gemeinschaft
Deutscher Forschungszentren (HGF)

ISSN 0947-8620

Abstract

A detector system for directional and time correlation measurements of multiple cosmic muons has been set up within the extensive air shower experiment KASCADE. The system consists of two layers (129 m² area each) of position sensitive multiwire proportional chambers (MWPC) triggered by a layer of segmented plastic scintillation counters placed upon an iron/concrete shielding above the MWPCs. Operation conditions and performance of the MWPCs have been studied by means of a prototype arrangement consisting of a stack of four detectors and two trigger layers. Results of the detailed prototype studies are presented and discussed. In particular, it has been found that for the present purposes an operation with a commonly used argon-methane gas mixture instead of previously used argon-isobutane leads to an excellent performance.
The chambers are integrated into the KASCADE experiment as described and are in continuous operation since 1996. Some typical measurements with the full detector assembly are used to illustrate which features of extensive air showers can be studied.

Die Vieldraht-Proportionalkammern im Zentraldetektor von KASCADE

Zusammenfassung

Im Experiment KASCADE zur Untersuchung ausgedehnter Luftschauer wurde ein Detektorsystem für Richtungs- und Zeitkorrelationsmessungen atmosphärischer Myonen aufgebaut. Das System besteht aus zwei Lagen ortsempfindlicher Vieldraht-Proportionalkammern von jeweils 129 m² aktiver Fläche. Die Kammern werden von einer Lage segmentierter Plastik-Szintillationszähler getriggert, die oberhalb einer Beton/Eisen-Abschirmung positioniert ist.
Die Betriebseigenschaften und Leistungsfähigkeit der Kammern wurden mit Hilfe einer Prototyp-Anlage untersucht, die aus einem Stapel von vier Detektoren und zwei Triggerlagen bestand. Die Ergebnisse der Prototyp-Studien werden vorgestellt und diskutiert. Insbesondere wurde erkannt, dass für den vorgesehenen Zweck ein Betrieb der Kammern mit einer gebräuchlichen Gasmischung aus Argon und Methan anstelle des früher genutzten Argon-Isobutan ausgezeichnete Eigenschaften der Kammern ergibt.
Integriert in das KASCADE-Experiment sind die Kammern inzwischen seit 1996 kontinuierlich in Betrieb. Einige typische Messergebnisse mit dem vollständigen Detektorsystem illustrieren, welche Eigenschaften ausgedehnter Luftschauer damit untersucht werden können.

PACS: 07.05.Hd; 07.50.Qx; 29.40.-n; 96.40.Pq

Keywords: Multiwire proportional chambers, Data processing, Extensive air showers, Cosmic muons

1. Introduction

Studies of high-energy muons in extensive air showers (EAS) are an important source of information about the energy, the nature, and the interactions of the primary cosmic particle inducing the EAS. The muons originate mainly from the decay of pions and kaons which are generated in the interaction cascade initiated by the primary particle. The measured characteristics of the EAS muon component, which becomes more sensitive to the parameters of the hadronic interaction with increasing energy of the observed muons, provide important shower parameters, which can be correlated with the observables of the other components and do most significantly contribute to infer the information about energy spectrum and mass composition of high-energy primary cosmic rays by EAS observations.

From the very beginning of the EAS experiment KASCADE (KArlsruhe Shower Core and Array DEtector) [1] set up on the site of the Forschungszentrum Karlsruhe (Germany , 110 m a.s.l.) great efforts have been made to install various different muon detection systems to measure (by use of different detection techniques) the lateral distribution and intensities of the muon component at different muon energy thresholds and to correlate the information of characteristic muon observables in an event-by-event mode.

One of these muon detection systems of KASCADE is an arrangement of 32 large-area multiwire proportional chambers (MWPC), which are installed as part of the KASCADE Central Detector [2] below the iron sampling calorimeter in two layers of 129 m^2 area each. The iron and concrete shielding above the MWPC arrangement effects an energy threshold of about 2.4 GeV for the detected muons. The MWPC have been originally designed by CEN Saclay and used in the accelerator experiment CELLO [3] at the PETRA e^+-e^- storage ring of the DESY laboratory. From there they have been taken over for the KASCADE experiment. While the mechanical layout has been essentially maintained, the electronic readout has been completely modernised and adjusted to the more stringent requirements in reliability, power consumption and stability of the long-term KASCADE experiment. In addition the gas supply has been changed from the originally proposed argon-isobutane mixture to a more convenient (and much less expensive) argon-methane mixture, for which favourable operation conditions could be found.

The operation of the MWPC has first been studied with a prototype stack in the laboratory [4,5,6] exploring the operation conditions and optimising the performance under the expected environmental conditions. We report about the results of the prototype studies and describe

the final assembly and operation of the MWPC detector component within the KASCADE experiment illustrated with some applications studying EAS features.

2. The chambers

2.1 General design

The 32 MWPCs have the same general design and are available in three different sizes as described in table 1. For the prototype studies chambers of type II had been used.

type	Number of chambers	total length (cm)	total width (cm)	number of anode wires	active area (m^2)
I	10	403	289	208	9.38
II	14	403	266	192	8.66
III	8	266	266	192	5.33

Table 1: Characteristic features of the MWPCs

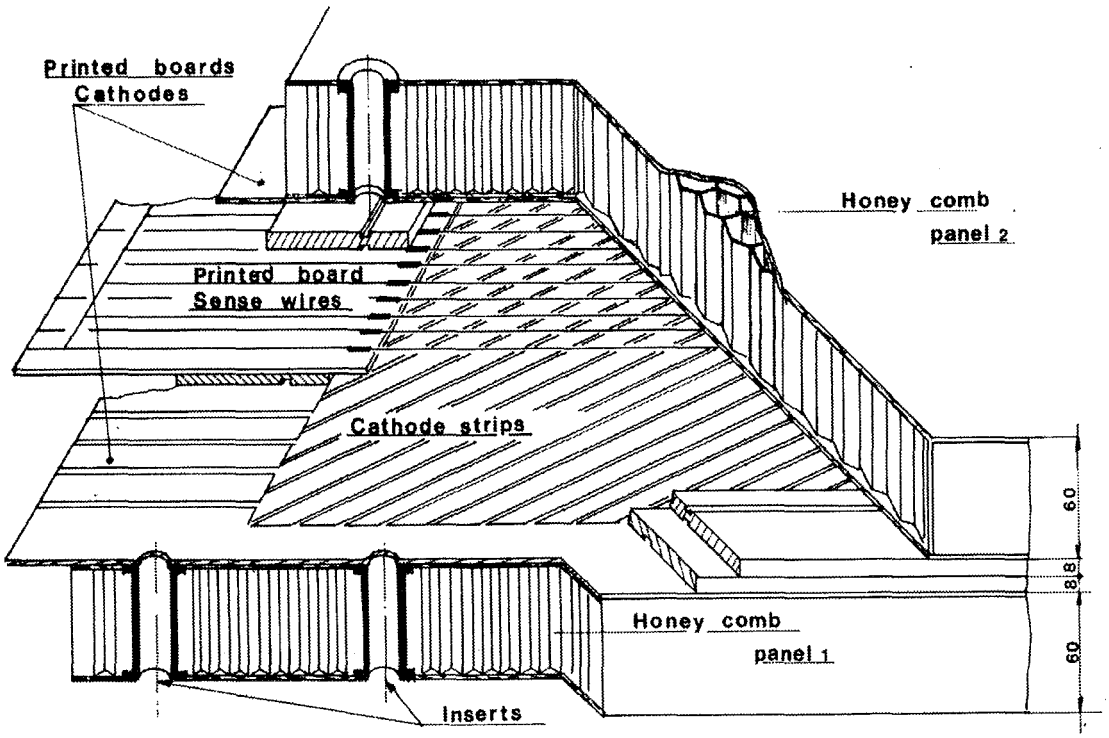

Fig. 1: *Mechanical construction of the chambers* [3]

The general layout of the chambers is schematically shown in fig. 1. In the centre of the 16 mm high active gas volume the anode wires are placed consisting of 20 µm thick gold plated

tungsten wires. The distance between the anode wires is 12 mm and they are separated by gold-plated copper-beryllium potential wires of 100 µm diameter. The wires are connected to the readout electronics by printed boards. As cathodes 10.6 mm broad copper strips on a printed circuit foil are glued on the upper and lower cover panels of the chambers at an angle of +34 deg. or –34 deg., respectively, with respect to the anode wires. The gap between the cathode strips is 2 mm. Sufficient mechanical stability of the chambers at a low weight is achieved by a honeycomb construction.

2.2 Read out electronics

Owing to the goal of detecting minimum ionising particles the electronics of the MWPCs is designed for a purely digital read out (Figs. 2 and 3). All channels are amplified and compared with individually adjustable thresholds. The discriminator outputs are synchronised with the trigger gate by digital delay lines and are locally stored until read out.

The electronics for 32 channels (wires or strips) is grouped on so-called motherboards (Fig. 3) which are attached to the MWPCs. The signals from each channel are fed to 8 amplifier modules containing 4 discrete charge integrating amplifiers made in SMD technique. Using complementary transistors the design for anode or cathode channels, respectively, is nearly identical. The anode amplifiers have a sensitivity of 540 mV/pC whereas the cathode ones are five times more sensitive in order to make the output signals about as high as those of the anodes. A 4-fold comparator chip on the amplifier modules compares the charge integrated signals with given thresholds.

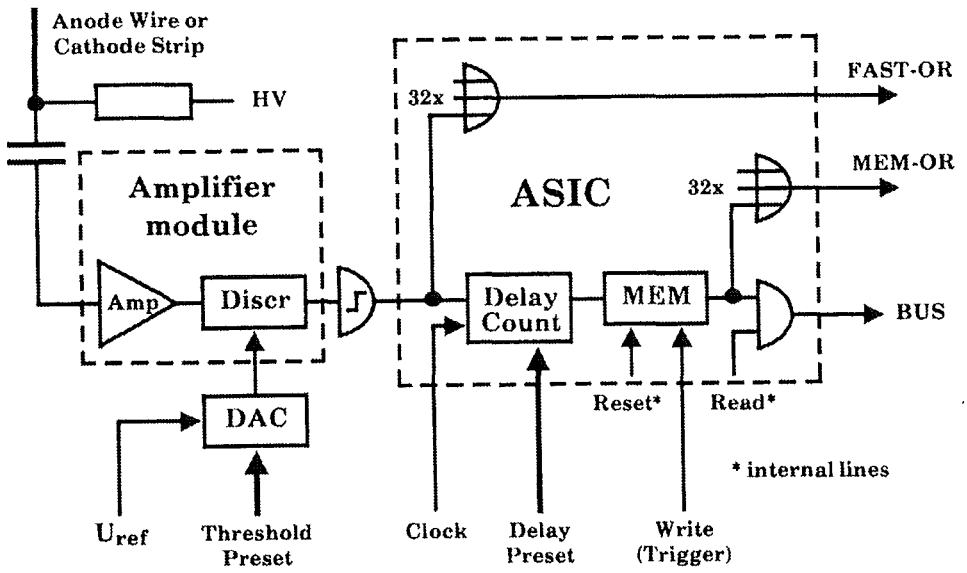

Fig. 2: *Electronic scheme of one read-out channel*

The digital signals are fed to 7 bit counters with preset operating at 40 MHz clock frequency thus providing the digital delay. With each new pulse the counters start counting downwards from the preset value to zero before the signal is transmitted further. Thereby, an individual delay is provided for each motherboard in order to compensate signal delay differences with respect to the trigger electronics between the front and rear side of the chambers and between different chambers. The outputs are gated by the central trigger signal and latched.

All 32 counters with their common preset register, the latches, and an interface for a (private) 8 bit data/address bus are realised in an ASIC. The threshold voltages for the comparators are generated with 8-fold 6 bit DAC circuits. These chips are accessed by the I²C bus [7], a special serial bus which, together with the private 8 bit parallel bus, forms the so-called 'local read-out bus' (LRB) of the MWPCs.

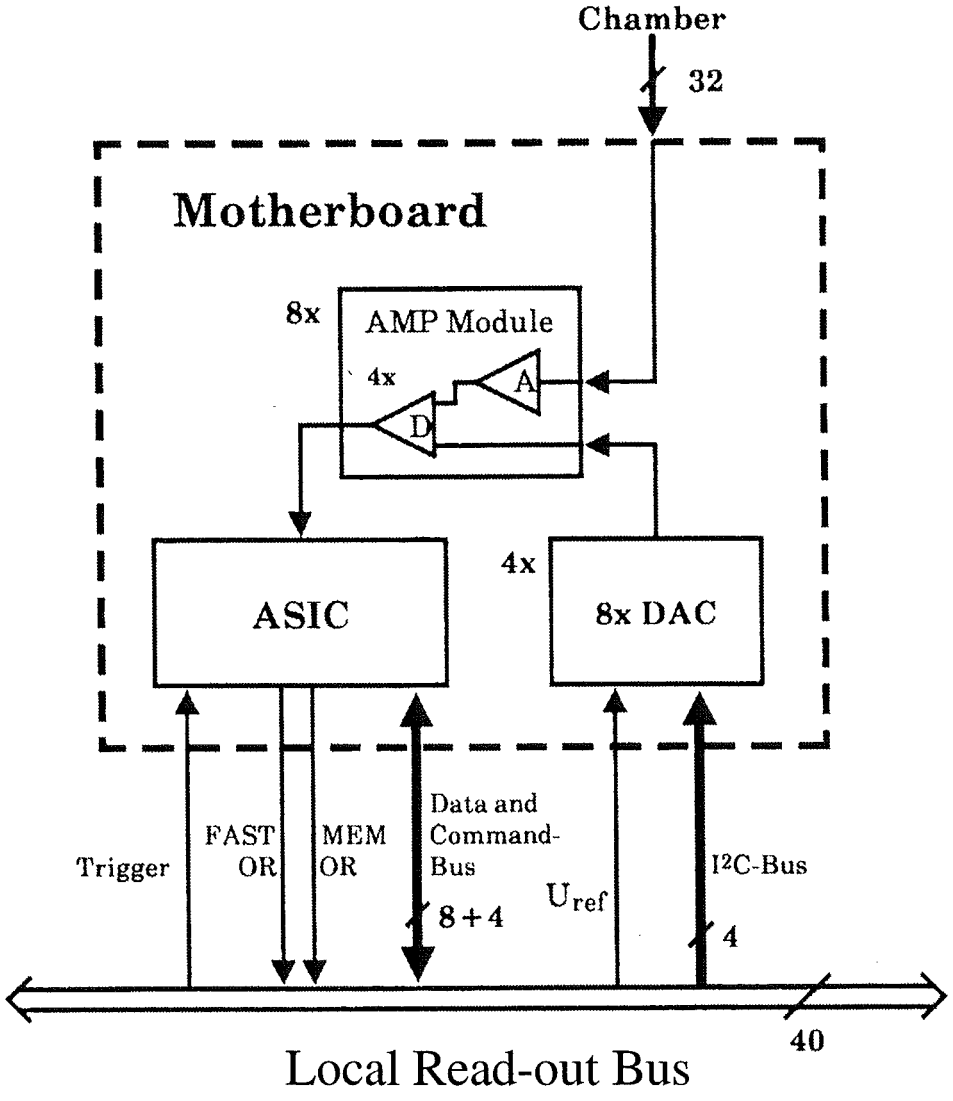

Fig. 3: *'Motherboard'*

One chamber contains 5 LRBs, two for the rear side (upper and lower cathodes) and three for the front side (upper and lower cathodes and anodes). In the prototype set-up the 5 busses are fed to a simple passive multiplexer providing a common bus of the same kind which is interfaced to the data acquisition system. In the final set-up operated in the KASCADE experiment active multiplexers controlled by T800 transputers are used. They access the LRB for parameter control and data read-out. The data of different chambers are then linked to a transputer based event builder via optical fibres and sent to the main KASCADE event builder located on a UNIX workstation [8].

2.3 Gas supply

The MWPCs are operated with a continuous flow of counting gas. The chambers are supplied in parallel with a flow rate through each chamber of about 3 litres per hour leading to an overall flow rate through all 32 chambers of 100 *l*/h. The pressure inside the chambers is adjusted to 3 mbar above the outer atmospheric pressure. Before the gas passes through the chambers an adjustable amount of alcohol vapour is added.

In the original arrangement at the CELLO experiment a mixture of argon and isobutane at a ratio of 67/33 vol. % was used. Therefore, the gas supply system of the MWPCs for KASCADE was also designed to mix argon and isobutane [9]. However, as will be shown below, during the prototype studies it turned out that the detectors could as well be operated by a mixture of argon-methane available readily mixed from factories. Thus, the system actually used in the KASCADE experiment and described here does not use all possible features of its design. Especially the security system is run in a simplified way.

The counting gas is supplied in packets of 12 bottles with 50 litre content each at a pressure of 200 bar. Two packets are available in a storage room and are plugged in parallel to an automatic switching device alternatively connecting one of the two packets to the gas flow controller without interruption of flow (Fig. 4 a)). If both packets are empty an alarm signal is generated.

In each branch of the switching device there are two different pressure sensors (Fig. 4 b)). One of them is a mechanical contact manometer and provides the signal of "full" or "empty at a level of < 5 bar". The other one, which is an electronic sensor, gives the filling status of the packet in bar. A pressure-reducing valve keeps the output pressure of the packet at a constant value of 3 bar independently of its actual content. An electromagnetic valve controlled by an electronic switching device switches the branch on and off. In addition to the automatic

switching mode there is the possibility to switch manually to one of the storage packets or switch off both of them.

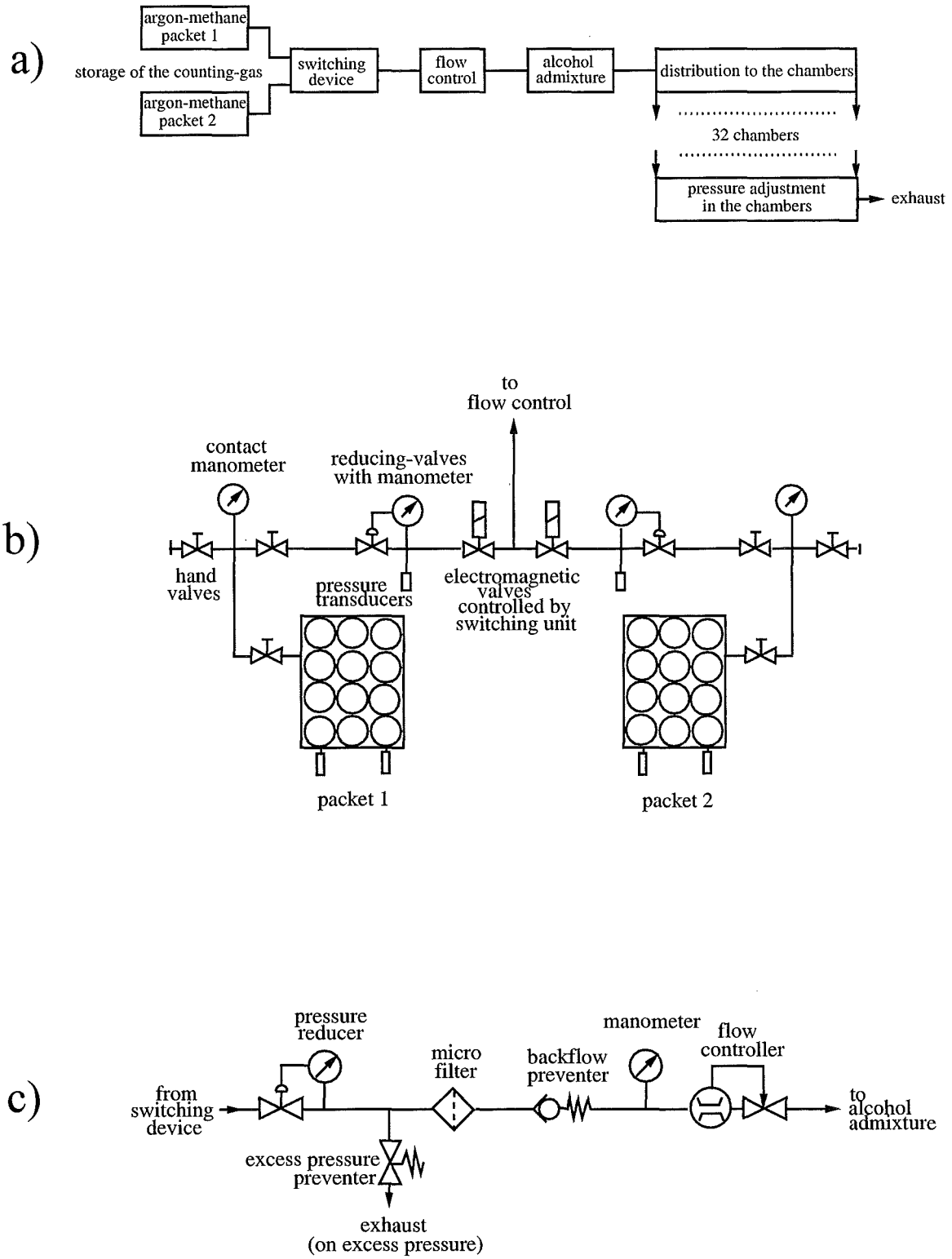

Fig. 4: *Scheme of the gas-supply system: a) general view, b) storage and switching device, c) flow control*

In a copper pipe coming from the gas storage room the counting gas enters the detector room where it passes a further pressure reducer. It keeps a constant pressure of 1000 mbar above the current atmospheric pressure independently of the filling conditions of the storage. This is needed to get the flow controller correctly working in its calibrated pressure range. After an excess pressure preventer, a micro filter, a backflow preventer, and a manometer the gas enters the flow-controller (Fig. 4 c)). This is adjusted to a flow rate of 100 *l*/h.

Before being distributed to the chambers the counting gas passes through a device, where it is saturated with a vapour of isopropyl alcohol at an adjustable temperature.

The distribution of the gas to the chambers is provided through a main pipe, where the pressure is kept at 250 mbar by a pressure controller, and a chain of 32 manual flow controllers. Each line to one chamber has a separate control valve to tune the individual flow resistivity and adjust a flow rate of about 3 *l*/h. In all lines to the chambers paraffin oil bubblers are mounted in parallel, which act as security valves for the chambers preventing gas pressures higher than 5 mbar above air pressure.

The counting gas passes the 32 chambers in parallel and flows back in individual lines to 32 paraffin oil bubblers, which keep the pressures in the chambers at 3 mbar above atmospheric pressure constant by the deepness of their glass-pipes dipping into the paraffin oil of 10 mm. The out bubbling gas is collected in the paraffin oil boxes and guided into the exhaust pipe.

2.4 Prototype arrangement

For studying the operation and optimising the performance of the chambers a prototype set-up has been assembled consisting of a hodoscope of four chambers of type II mounted horizontally one upon the other with a distance of 60 cm between each other [5]. In the gaps between the uppermost and second chamber and the third and lowermost chambers, respectively, segmented layers of plastic scintillation counters for timing and triggering have been installed. For shielding against the soft electron/gamma EAS component layers of 12 cm iron and 10 cm lead carried by concrete walls have been placed on top (Fig. 5). This shielding of 25 radiation length leads to an energy threshold of about 0.4 GeV for muons traversing the hodoscope vertically. The whole set up has been mounted inside a light weight constructed experimental hall protecting against weather influences. A constant air conditioning, however, has not been provided.

The modules of the trigger device are based on scintillator material NE 114 (polyvinyltoluol) of 3 cm thickness. The 8 modules of the upper plane contain two scintillator plates of 47.5 ·

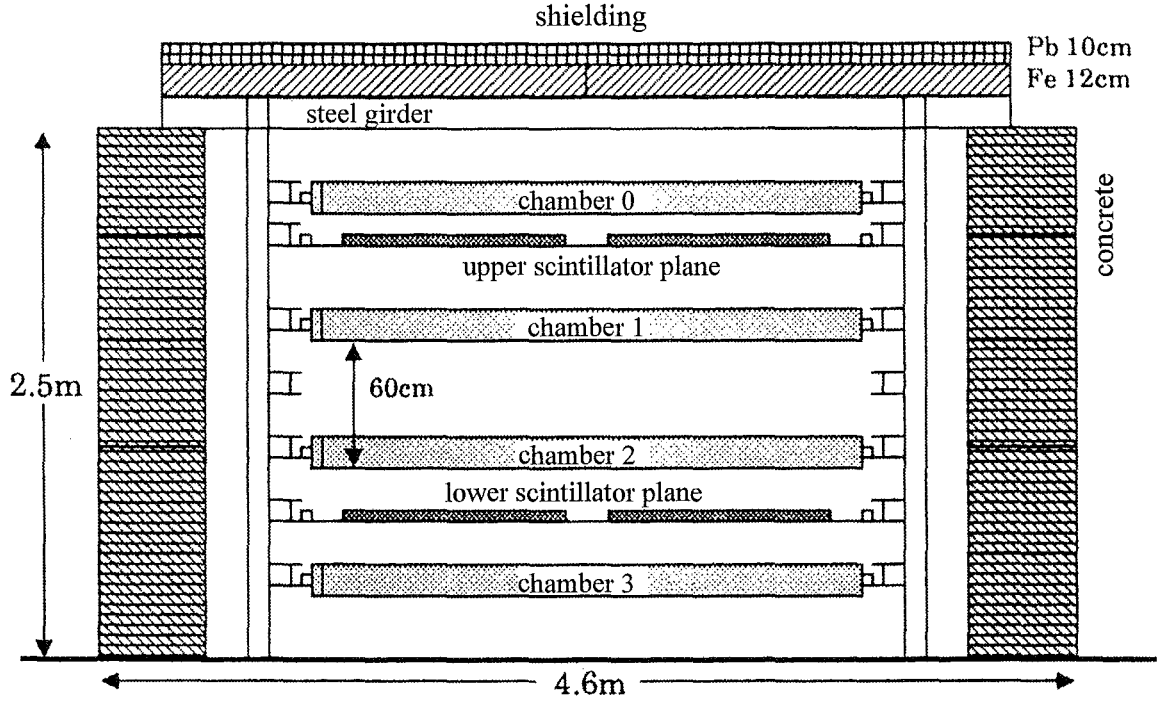

Fig. 5: *Schematic view of the prototype arrangement*

96 cm² size each and the 8 modules of the lower plane are built up by four plates of 47.5 · 47.5 cm² resulting in sensitive areas of about 7.3 m² each. The light collection is done via wavelength shifters of NE 174. In the upper trigger modules rods of about 1 m length are placed in the middle between the scintillator plates and are read out from both sides by 1.5" photomultiplier tubes (EMI 9902). In the modules of the lower plane rods of half this length are put between each pair of the plates and are read out on one side only. The two pairs of scintillators in this plane are optically separated hence forming two independent counters.

The trigger electronics is composed of standard nuclear electronic modules. The signals from the optically not isolated photomultipliers of the upper trigger plane are added in analogue way by linear fan-in/fan-out modules (Le Croy 428F). Their outputs as well as the signals from the lower trigger plane are fed into constant fraction discriminators (CF 8000) which also perform a logical OR of each 8 inputs. The master coincidence is formed by a coincidence of the ORed outputs of all modules from the lower trigger plane with the ORed outputs of all modules from the upper plane.

For the time measurements the multiple time digitizer ARTS (ARrival Time System) has been developed (Fig. 6). Using standard electronic components ARTS features with a reasonable resolution by a simple, compact, and low cost layout. ARTS records continuously in steps of 20 ns the time history of 32 input channels for an overall time of 5.12 μs. If a trigger signal appears the history is stored in memory. The output signals of the constant fraction

discriminators serve as inputs for ARTS. Using ECL-TTL converters (Motorola MC10125) the NIM pulses are converted to TTL level and fed into RAMs (Cypress CY7C123). The static RAMs cover 256 bit with a width of 32 bit. The addresses of the RAMs are generated with two synchronous counters (74F191). A quartz oscillator of 50 MHz is used as clock. On one edge of the clock signal the counter is incremented and on the second edge the RAMs are strobed. A trigger stored by a flip-flop (74F74) stops the counter and inhibits further writing to the RAMs. For read-out the counting direction of the counters is reversed and the RAMs are connected to a private 8 bit data and 2 bit address bus. An access on the last byte increments automatically the RAM addresses. After read-out the module is reset by a simple write access.

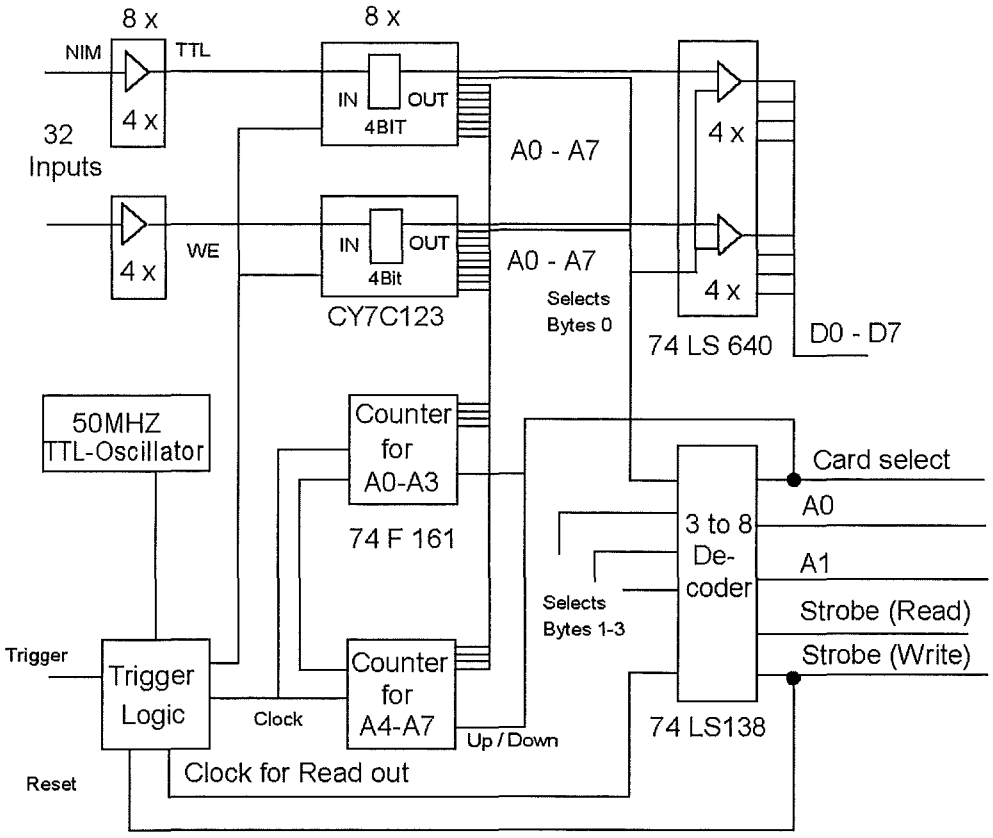

Fig. 6: *Block diagram of the arrival time measuring system ARTS*

In case of the prototype set-up the data acquisition is based on 4 interface cards to different bus sub-systems controlled by a personal computer (PC). The first sub-system is a home made interface to couple the multiplexed 'plane bus' of the MWPCs to the bus of the PC. It allows to access all plane multiplexers of the four MWPCs on the same bus. The second sub-system is again a simple home made interface to the private bus of ARTS. The third sub-system is a CAMAC crate coupled to the PC by a Struck PC1331/Turbo interface. The CAMAC system is used for a fast gate module to lock the trigger and for some scalers, ADC- and TDC-

modules. Integrated in the CAMAC system is also the interface to the high voltage supply consisting of two CAEN SY 127 crates. The fourth sub-system is an IEEE 488 bus connected to the PC by a Keithley PC488 interface.

As software the multiparameter acquisition and control program package MYDAS has been developed [10]. In order to fit the inhomogeneous bus and interface hardware the program is designed extremely modular in 36 modules for different tasks. For future system changes and for portability the package has a layered structure and is programmed in ANSI C. All hardware or operation system dependent calls are concentrated and encapsulated in special layers of the software. In particular, also simple graphical commands are interfaced to MYDAS by special, well defined calls. Besides the raw experiment control and data acquisition MYDAS provides various event displays including on-line rotatable 3-dimensional views of the detector assembly and it performs the complete analysis of data.

The analysis is split into two main groups. The first group contains all analyses which are based on a single MWPC or any other single component of the system, like channel maps, hit reconstruction and hit classification. The second performs all analysis based on the information of multiple detector components, like the reconstruction of particle tracks, association with arrival time and various efficiency controls.

The first level of analysis provides channel maps and multiplicity spectra for all different planes of the MWPCs which proved to be very useful for identification of broken wires and electronic problems. Multiplicity means the number of wires or strips of one plane involved in one event. This quantity is especially useful for adjusting the parameters of the chambers because it reflects somehow the charge distribution in the chamber and, therefore, gives information about the gas amplification.

Additional information about the quality of the MWPCs comes from a classification of patterns for single hits. In the different classes all possibilities of chamber information are sorted. Starting from no data, only a single anode, anode and cathode etc, to the expected pattern of a hit, with anode, lower and upper cathodes intersecting in a small area. Different groups of classes therefore indicate missing efficiency of one or more physical planes of the chambers.

For reconstructing the hits in a MWPC two sets of intersections are collected from all intersections of the anodes with either of the two cathode planes. Spatially close points from both groups are taken as hits by averaging the coordinates of the two points.

The second level analyses, based on the combined information of all chambers, starts with the

reconstruction of the tracks. All combinations of either 4 or 3 hits are stored in different lists. To all 4 point hit tupels a linear fit is applied in two projection planes. A track is accepted when the maximum distance of none of its points to the fitted line is more than 4 cm. If two tracks have more than one point in common, the track with the largest distance to one of its points is rejected. Combinations of 3 points are treated in the same manner. However, when a track based on four points has more than one point in common with a track based on 3 points, the 3 points track is always rejected.

For all tracks based on 3 hits only it is calculated whether or not the track passes the missing chamber. This gives a direct estimate of the efficiency for the chambers. The distances of the points to the fitted track are accumulated for each chamber in x- and y-directions, respectively.

The association of the tracks with the arrival times in the scintillators is not in all cases unambiguous. Therefore, a list of all time track combinations is constructed and analysed on base of the highest probability.

3. Operation and performance

3.1 General adjustment

The adjustment of the free operational parameters like signal delays, discriminator thresholds and high voltages is done for each chamber separately, based on the first level analysis described above. For a given gas mixture the high voltages and the thresholds are set to reasonable values for optimising the signal timing which is practically independent of the other conditions. The signal timing is adjusted by a series of short measurements of about 100 events in a first scan and 1000 events around the optimum. The optimum is defined by the highest fraction of events with an ideal event pattern. Repeating the procedure for different gate widths shows that the efficiency is increasing with the gate width up to a value of about 350 ns. For 400 ns and more a kind of saturation is observed (Fig. 7). For the MWPCs the first noisy channels are observed at gate widths larger than 1000 ns. The gate width of 1000 ns provides a sensitive time window for particle registration of 600 ns after the trigger signal. The threshold adjustment and the high voltage setting are more or less opposite parameters. Due to low signals at the cathodes these thresholds are set to the minimum value which is the lowest setting before noise appears. The larger signals at the anodes allow significantly higher thresholds.

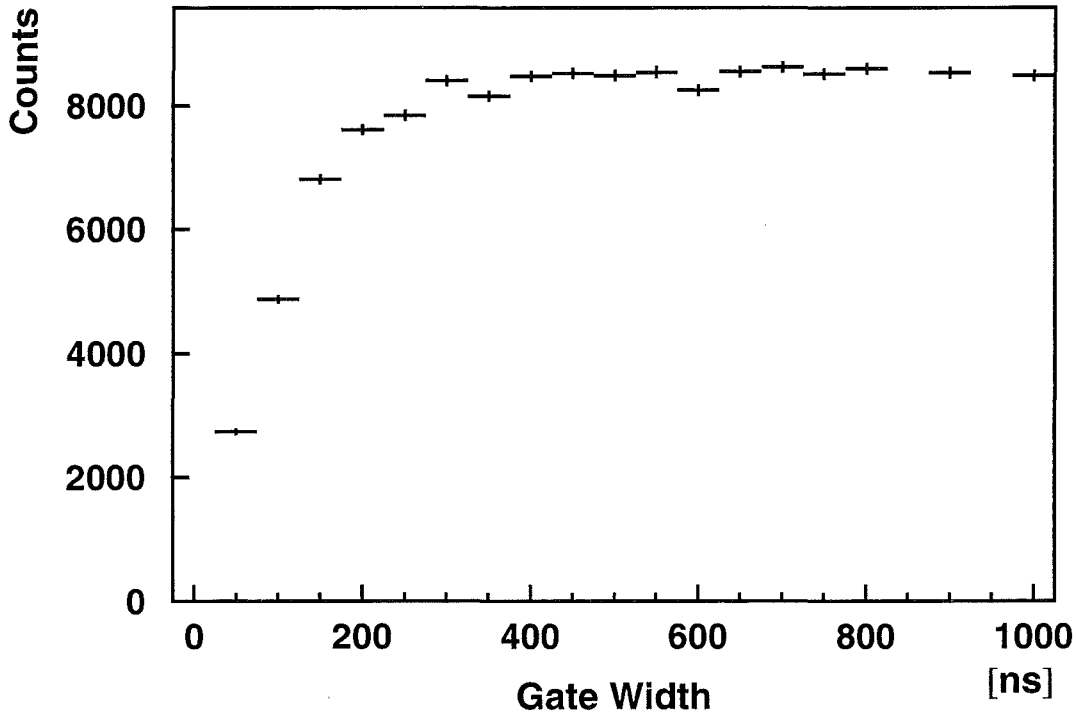

Fig. 7: *Efficiency of a single chamber versus gate width*

A systematic scan of high voltages for the anodes shows a fast increase of the efficiency when the chamber reaches the proportional region and a plateau region above. HV-setting at the lower end of the plateau proves to be an optimum because the probability for discharges increases rapidly with increasing high voltage. The voltages for the potential wires are set to reasonable values, again limited by the appearance of discharges. The influence of the potential wires is comparably small as can be seen from the multiplicity of the anodes. As the pulse heights from minimum ionising muons are close to noise pulses the choice of the gas mixture turns out to be a critical point of the operation.

3.2 Studies with different counting gases

As mentioned above in the CELLO experiment the MWPCs have been operated with a argon-isobutane mixture (volume 2:1), which is used in many experiments with proportional counters, too. The main argument for the use of argon-isobutane results from the relatively high specific energy loss, leading to a good energy resolution due to the high number of primarily created electron-ion pairs.

In the present application, the detection of minimum ionising particles, the requirements are slightly different. Because of the digital read-out the energy resolution is less important

whereas the total signal height plays the important role. Hence, a smaller ionisation might be compensated by a higher gas multiplication. However, in order to obtain high enough signals the MWPC are driven near the break down limit as concluded from the appearance of pseudo geiger and geiger pulses.

Due to the use of argon with its lowest radiative excitation of 11.6 eV it is necessary to have a good quenching at this energy. Methane fulfils this condition by its various absorption bands in this range. The quality of operation with the argon-isobutane mixture (2:1) and the argon-methane mixture (9:1) can be recognised best by comparing the spectra of multiplicities, in particular of the cathodes. The behaviour within typical ranges of voltages for each gas mixture is demonstrated in Figs 8 and 9.

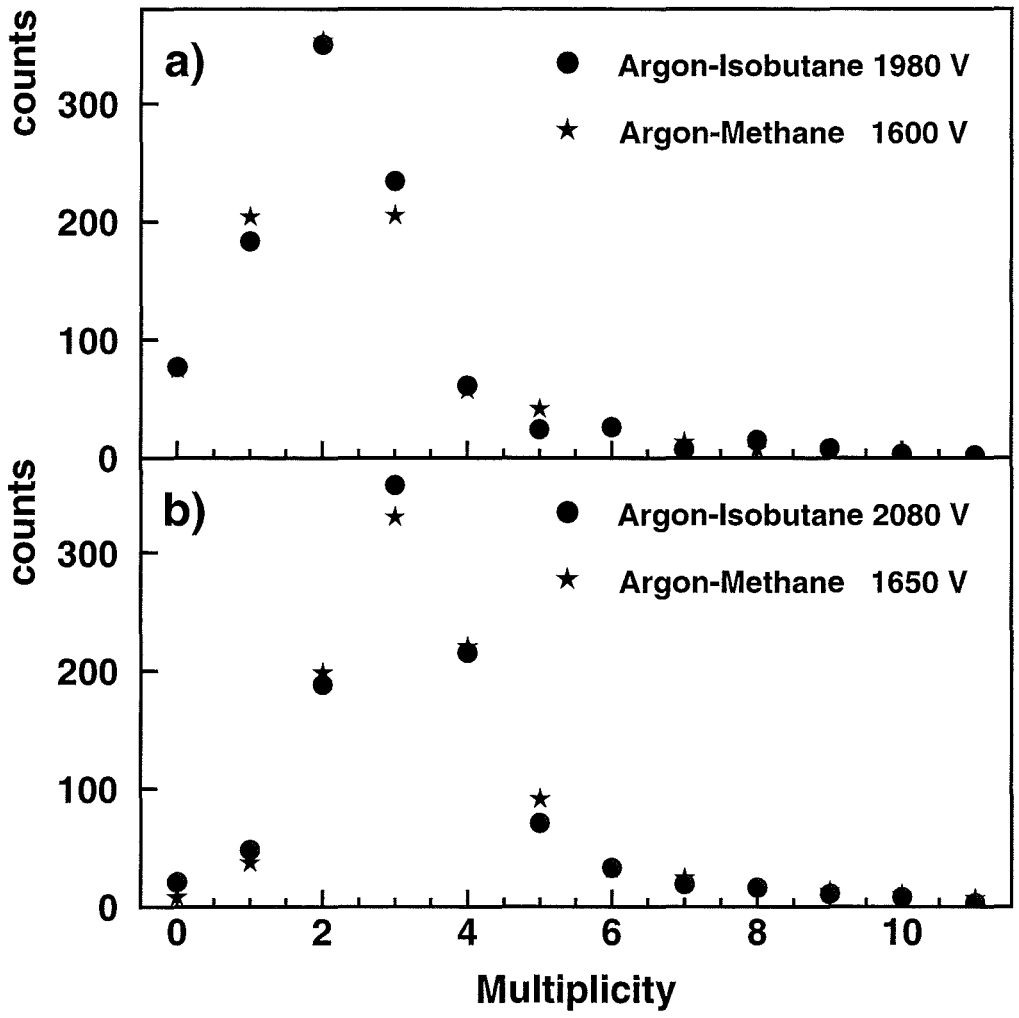

Fig. 8: *Distribution of hit multiplicities for different counting gas mixtures and high voltages*

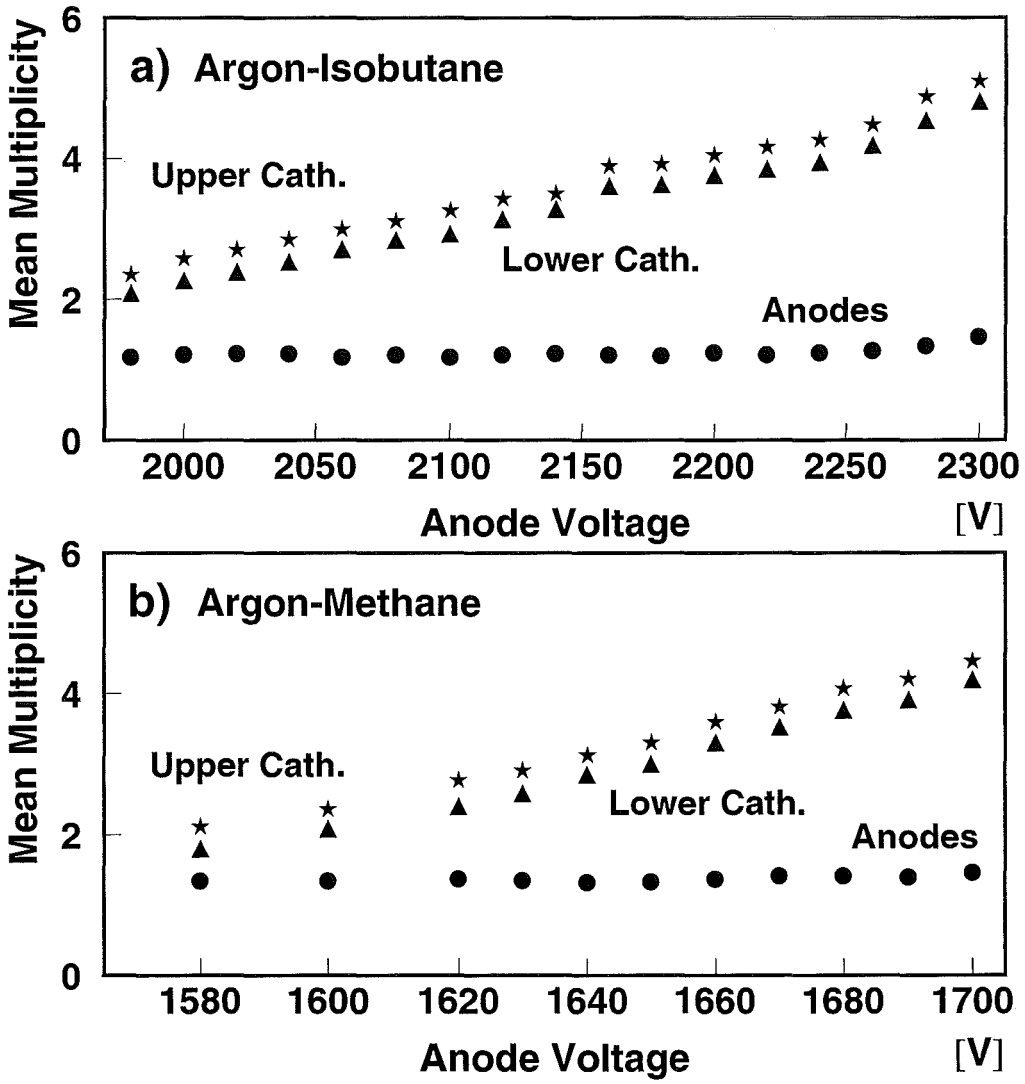

Fig. 9: *Mean multiplicities for different counting gas mixtures versus anode voltage*

It turns out that the voltage range of 1960 - 2300 V for argon-isobutane is comparable to the voltage range of 1570 - 1700 V for argon methane [6]. A setting of 1700 V is sufficient for argon-methane to run the detectors stable in the long term. Compared with argon-isobutane a lot of further arguments speak for the use of argon-methane, too. This gas is offered from factories at a comparably low price as readily mixed gas in the purity needed because it is widely used in monitors for radiation control and protection. Security requirements for the use of argon-methane are strongly reduced in comparison with argon-isobutane because it is neither explosive nor inflammable in that composition.

Since the gas pressure in the chambers is stabilised relatively to the air pressure the signals depend on it. Figure 10 shows the effect quantitatively by means of the measured multiplicities. From comparison with Fig. 9 it can be concluded that the maximal expectable

increase of the air pressure by 50 mbar can be compensated by a voltage increase of 20 V. This increase would always be possible because the proportional limit also increases with the gas pressure. Due to the smallness of the effect a control of the high voltage in dependence of the air pressure is not applied. Instead, the voltage is set to a reasonable value leading to a stable efficiency over the whole range of possible air pressures.

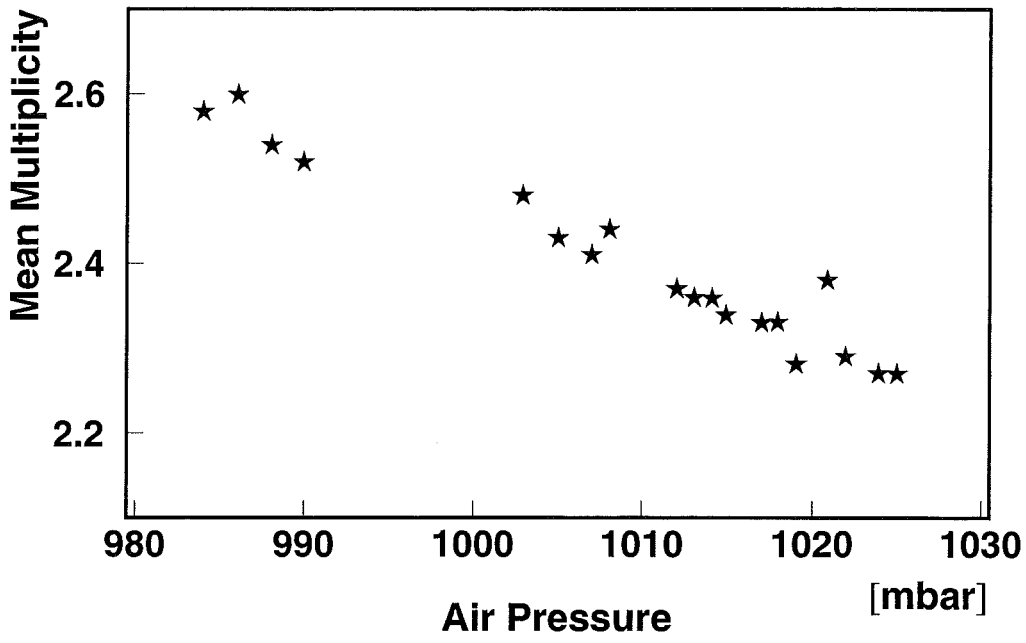

Fig 10: *Mean multiplicities versus air pressure for argon-methane mixture*

3.3 Performance of the prototype system

After the adjustment of the single detector components the prototype set-up is checked as complete detector system. The direction along the anodes is defined as y-axis, the direction cross the anode wires as x-axis. The origin of the coordinate system is set to a virtual point at the level of the lowest MWPC.

All chambers are assumed to be parallel to the coordinate axes. This is fulfilled by the construction of the frames within 0.2 deg.. The position of the detectors is known from the mechanical measurement with an uncertainty of 1 cm in x-direction and 2 cm in y-direction. Because these uncertainties are within the search limits of the tracking algorithms, the distance of the points in each MWPC to the fitted tracks can be used to make a relative position adjustment of the MWPC. Figure 11 shows a typical distribution of the hit distance to the fitted track the mean value of which is different from zero. The off-set value is not directly the mechanical shift of the chamber, because its possible mispositioning is included in the fit.

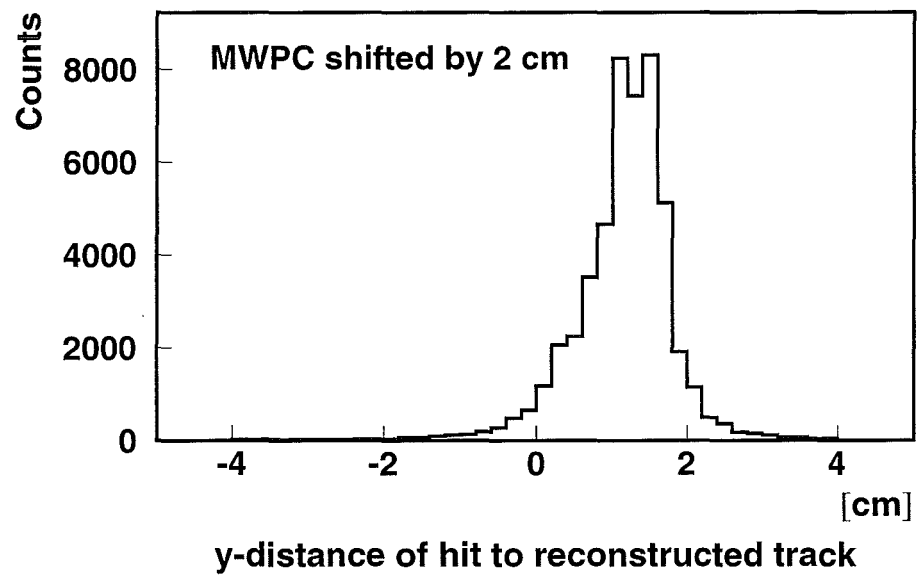

Fig. 11: *Distribution of the y-distances to the reconstructed track in one MWPC showing the effect of a displaced chamber*

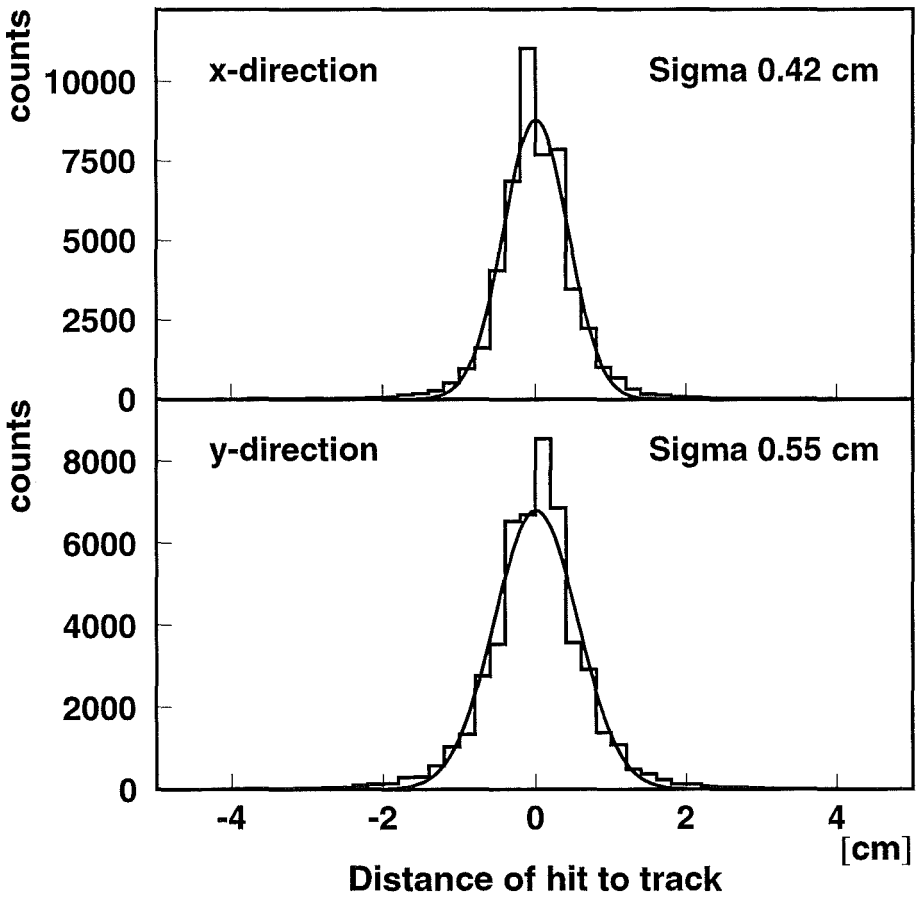

Fig. 12: *Distribution of the distances to the reconstructed track in x- and y-coordinate with fits for resolution*

Nevertheless, the value indicates the size of the shift and the direction. With an iteration procedure the relative adjustment of the chambers can be achieved with an accuracy of better than 1 mm. The distribution of the distances to the fitted track allow a direct estimation of the spatial resolution (Fig. 12). It turns out that the resolution in x-direction is 0.42 cm and in y-direction it is 0.55 cm. The angular resolution of the system is therefore depending on the azimuth angle but is about 0.15 deg., a value which is negligible in comparison with the angular scattering for muons in the GeV region in the shielding above.

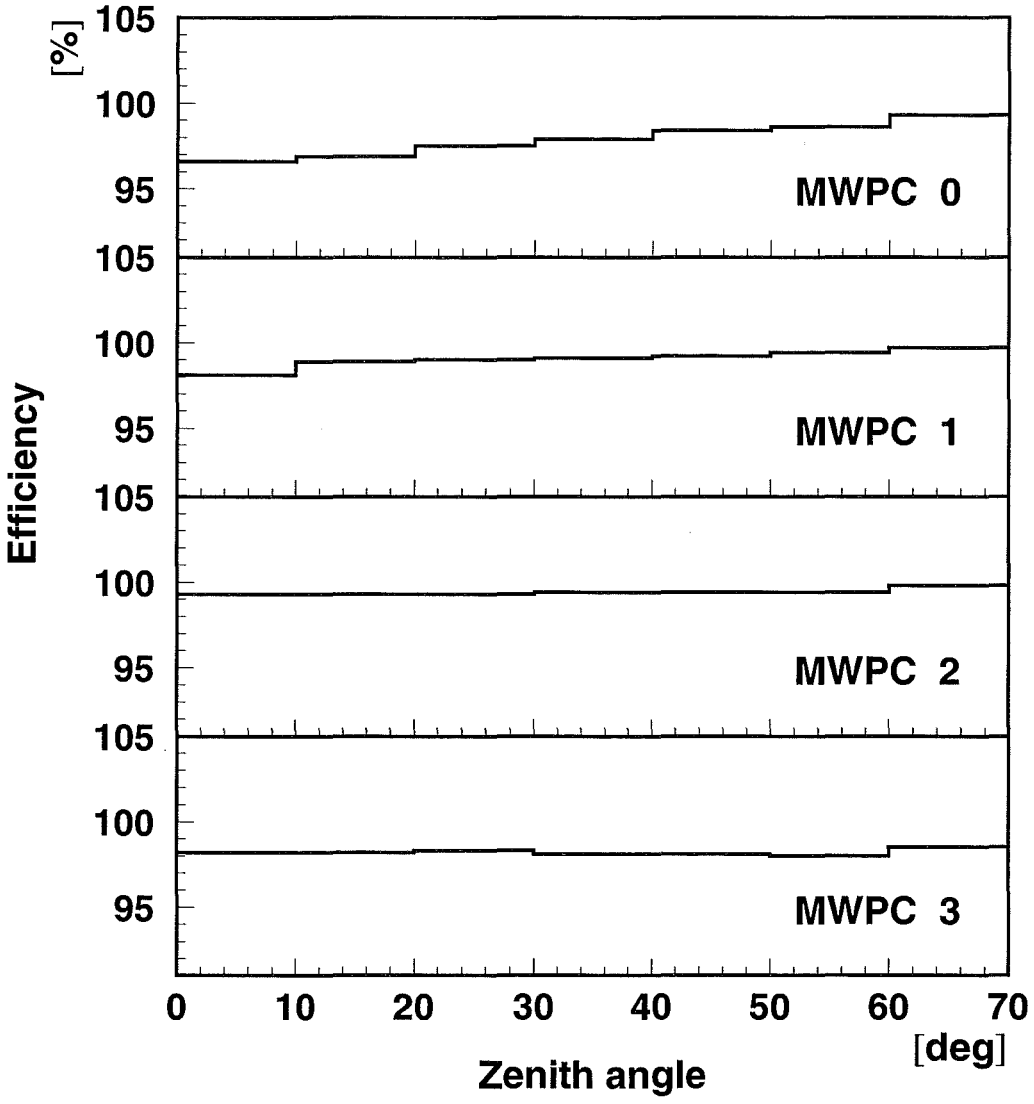

Fig. 13: *Efficiency versus angle of incidence*

An integral measurement of the chamber efficiencies yields values of 97.6, 99.0, 99.3, and 98.2% for chambers 0, 1, 2, and 3, respectively. The dependence of efficiencies on the zenith angle are shown in Fig. 13. The efficiencies are very stable over the complete acceptance of the system. Only towards $\Theta = 0$ deg. (equivalent to the shortest track in the gas) a slight

decrease is observed. An azimuthal dependence of the efficiency of the chambers has not been observed.

Fig. 14 shows a measurement for the efficiency of particles delayed to the triggering particle. The gate width of the trigger is set to 1000 ns. It turns out that the efficiency is stable within a time window of 600 ns after the trigger, in agreement with the results of Fig. 7.

4. Results of the prototype device

4.1 Flux of cosmic muons

Due to its high homogeneity with respect to efficiency and the high angular resolution the detector system suits well for measurements of the directional intensity and flux of cosmic muons. The directional intensity depending on the zenith angle Θ and the azimuth angle Φ is defined as

$$I(\Theta, \Phi) = dN / (dA\perp \cdot dt \cdot d\Omega)$$

with the particle number N, the perpendicular area $A\perp$, the time t and the solid angle Ω. The observable accessible by the experiment is the number of particles per zenith angle interval resulting directly from the reconstructed tracks. Due to the geometry of the set-up, the detector acceptance is depending on both, zenith and azimuth angle of incident particle.

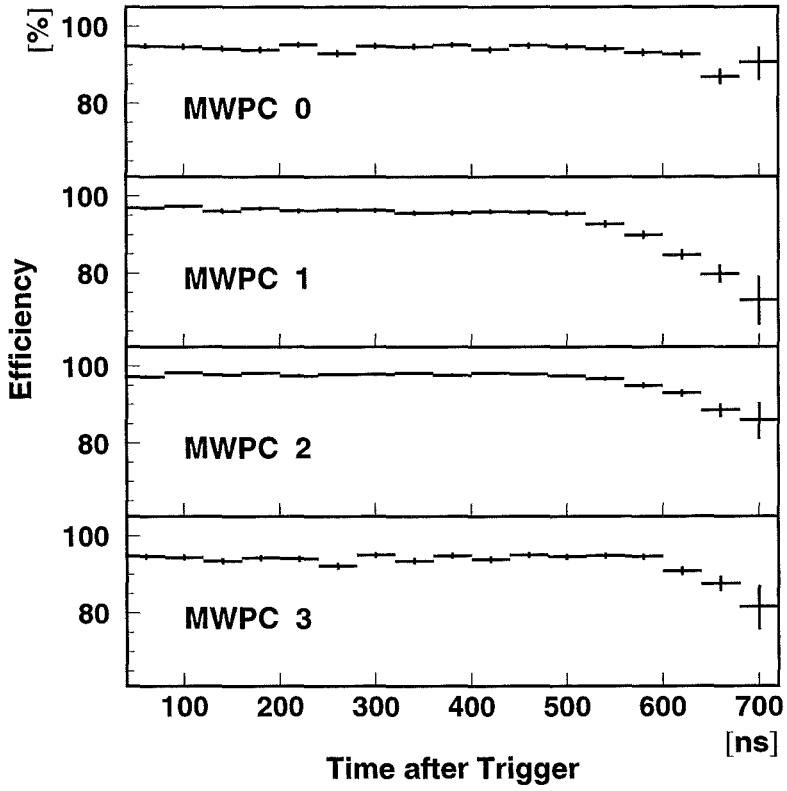

Fig. 14: *Efficiency for muon arrival times delayed to the trigger time*

Assuming a uniform distribution in azimuth the acceptance is determined by the Monte Carlo method, i.e. a correction factor for each zenith angle interval is obtained. Transferring $d\Theta$ into $d\Omega$ and dA into $dA_\perp$ by division of $\sin\Theta\ \cos\Theta$ the relative directional intensity of cosmic ray muons integrated for $E_\mu > 0.5$ GeV (the average threshold) is deduced. Figure 15 shows the result combined with a fit of $I(\Theta) = \cos^n \Theta$ with an index $n = 2.02 \pm 0.08$. This result agrees within 1 σ with the mean value compiled by Bhattacharia [11]. Compared with a result at a similar threshold of $n = 1.98^{+0.07}_{-0.03}$ [12] the agreement is very good.

A comparison of the simulated directional intensity with the measurements shown in Fig. 16 proves the way of analysis, as well as the assumption of isotropy in the azimuth angle. The

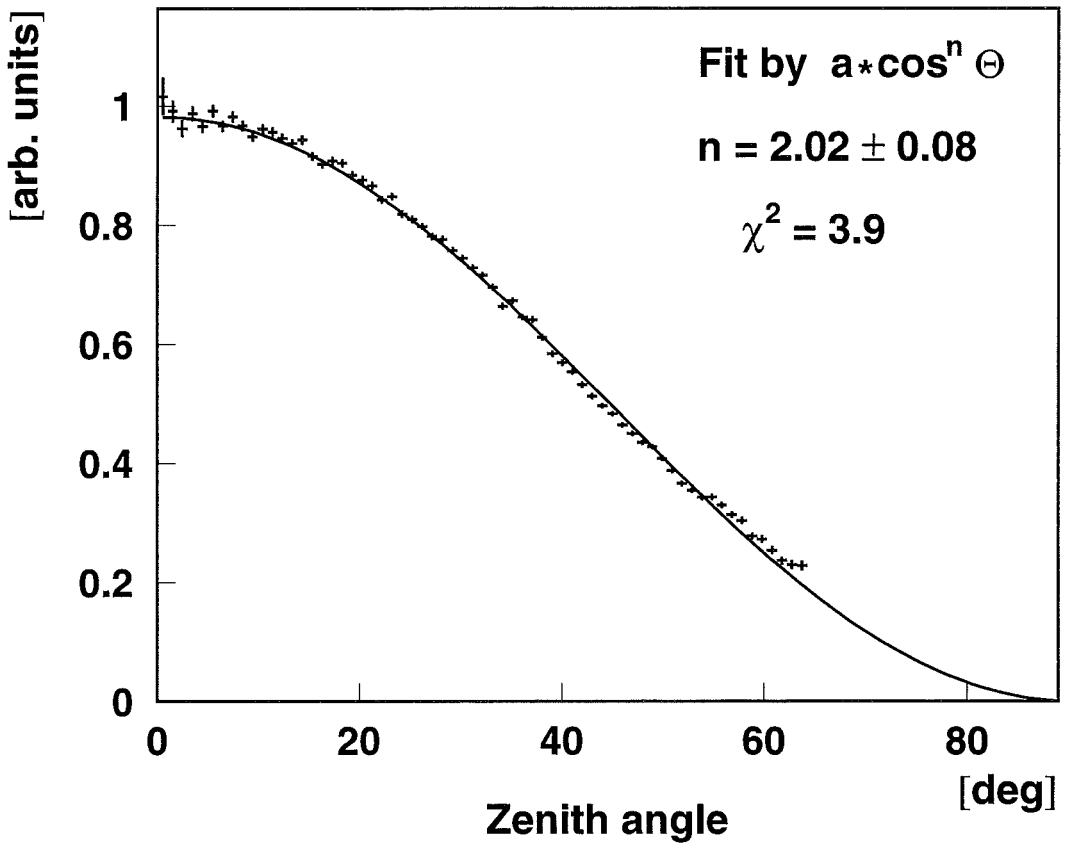

Fig. 15: *Directional intensity of muons fitted by $a \cdot \cos^n \Theta$ [5]*

lack of measured particles at $\Phi = 160°$ results from a building adjacent to the experimental hall in this direction.

From the Monte Carlo results the total correction factor for the acceptance of the hodoscope between the measured rate and the flux J1 of muons traversing in a downward sense a horizontal area element defined by:

$$J1 = \int I(\Theta,\Phi)\cos\Theta \; d\Omega$$

The flux is corrected for the dead time of the acquisition system and for the particular efficiencies of all MWPCs and all trigger modules. Further corrections are made for the dependence on atmospheric conditions using the recently measured coefficients -1.7% /mbar and -0.11% /°C [13] resulting to

$J1 = 133.1\ m^{-2}\ s^{-1}$ for $E_\mu > 0.5$ GeV

at a temperature 0° C and a pressure of 1013 mbar. Using the measured directional intensity

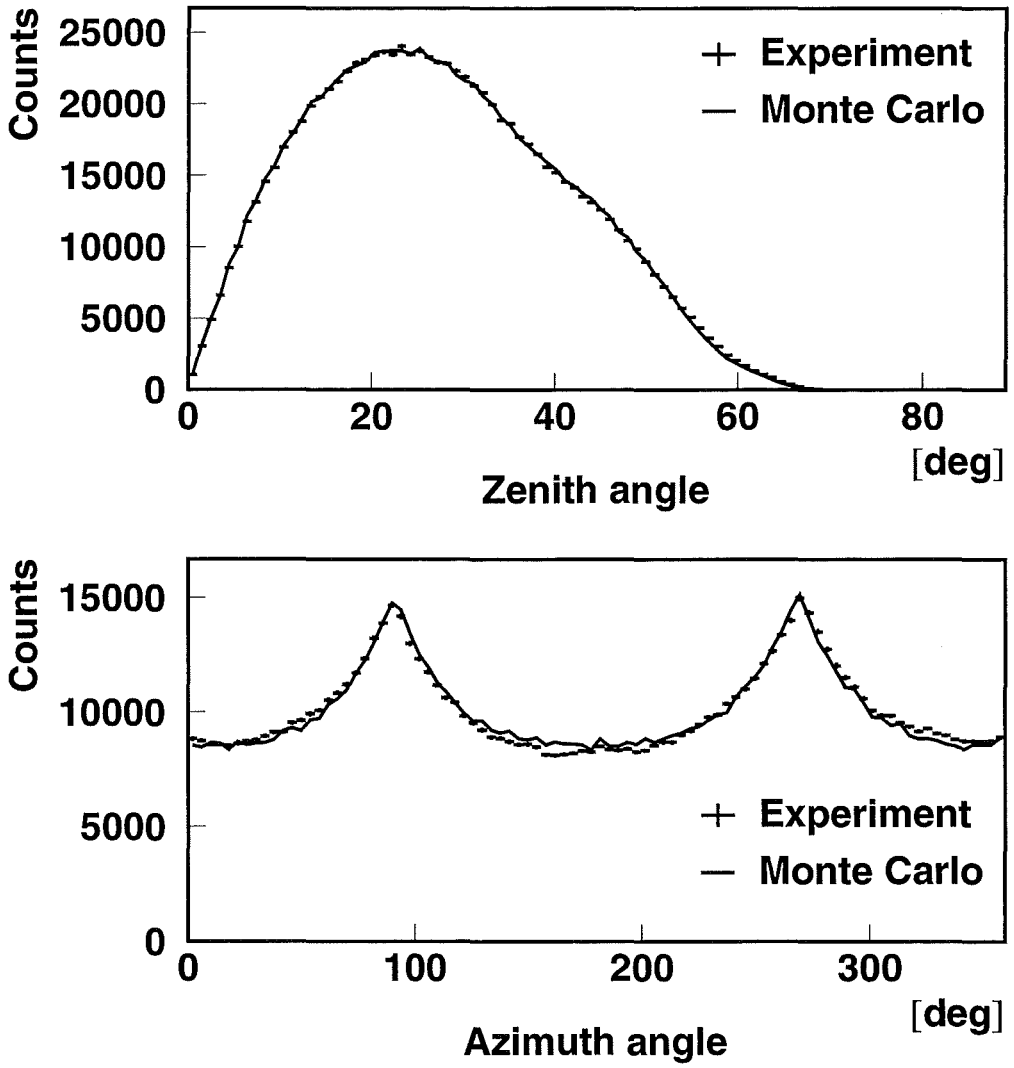

Fig.16: *Measured zenith and azimuth distributions compared to Monte Carlo calculations [5]*

the omnidirectional intensity

$$J2 = \int I(\Theta,\Phi)\, d\Omega = 177.2 \pm 4.8\ m^{-2}\ s^{-1}$$

and the vertical intensity

$$I(\Theta = 0) = 85.2 \pm 3.4\ m^{-2}\ s^{-1}\ sr^{-1}$$

is deduced.

These measurements of the directional intensity and total flux prove the high quality and stability of the set-up measuring directions of muons.

4.2 Muon charge ratio

The prototype detector arrangement enables to study the decay of stopped muons since the lower trigger plane is placed above the lowest MWPC. The general signature for the decay of a muon is the observation of a track in the three upper proportional chambers accompanied by the appropriate signals in both trigger planes and a missing hit in the lowest chamber. From the decay spectrum the ratio of positively to negatively charged atmospheric muons can be derived.

Positively charged muons decay with a time constant like free muons (in flight) of τ_{μ}^{+} = 2.19703 μs whereas the decay constant for μ^- is shorter depending on the material in which they have been stopped. The reason for this behaviour is the formation of muonic atoms in the stopping material opening a second weak interaction decay channel, namely the capture of the muon in the atomic nucleus, leading to an enlarged decay width and hence a reduced decay time constant. By use of the Fermi-Teller law it can be calculated that in the scintillator material polyvinyltoluol $[(CH_2CH(C_6H_4CH_3)]_n$ 84% of the muons are primarily captured by carbon atoms and 12% by hydrogen atoms. Due to molecular impact processes, however, which happen with a rate of 10^{11}/s most of the muons are transferred to the more attractive carbon atoms. Hence, with high confidence it can be assumed that muons are captured by carbon atoms only. Subsequently, the negatively charged muons may be captured by the atomic nucleus with a probability of 7.86% [14]. This does not lead to a signal in the scintillator since only neutral particles are emitted by the following weak processes. The residual 92.14% of muons decay with an effective time constant of 2.0263 μs [15].

Since the charge state of the muons is not identified in the experiment the observed decay constant results from a superposition of the values for μ^+ and μ^- leading to a decay time somewhere in between. The measured value is directly correlated with the muon charge ratio [5].

Due to the features of the time digitizer system ARTS the decay electrons can in principle be seen either in the MWPC below or above the stopping trigger detector if the decay happens earlier than 600 ns after arrival of the muon. A safer electron signal, however, comes directly from the stopping scintillator itself. Therefore, the identification of muons being stopped and decaying afterwards in the lower scintillator plane was performed by following cuts to the full data sample:

- The track determined from the upper MWPCs passes through the active area of the lowest chamber. However no hit is seen in the latter.
- In the lower trigger plane occurs a second signal in the detector module contributing to the trigger signal.
- One track only is observed in the detector system.
- One module only of each trigger plane responds.
- There are no further coincidences between the trigger planes within the time window of ARTS.

With these cuts also true decays were partly rejected. Concerning background, however, they were found to be best leading to signal/background ratio of $5 \cdot 10^5$. Therefore, a correction for background was omitted.

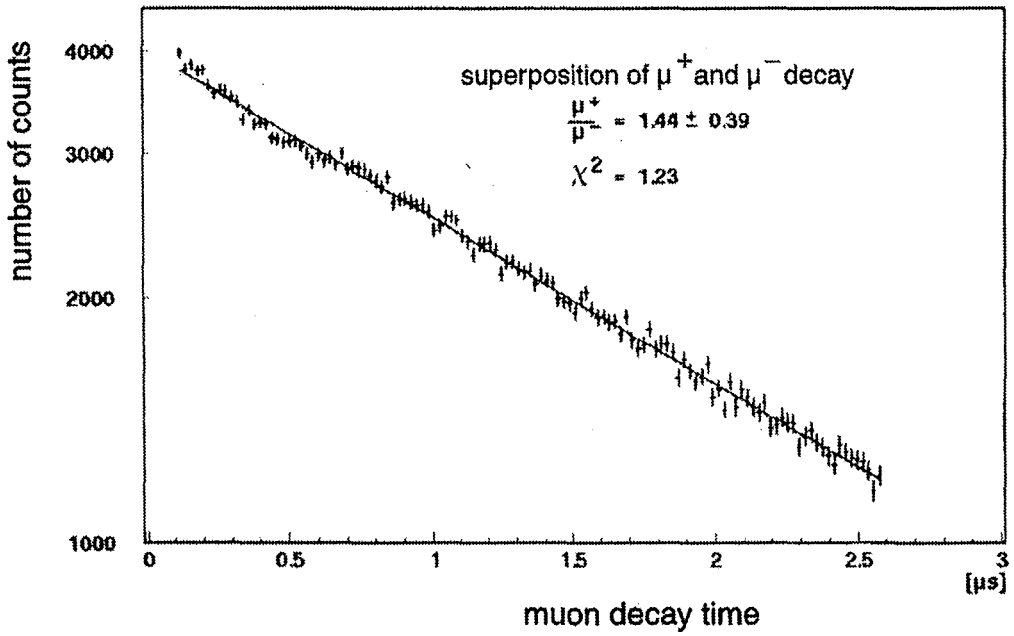

Fig. 17: *Superposition of the free decay of μ^+ and the decay of μ^- stopped in carbon fitted to the measured muon decay time spectrum [5]*

The measured time spectrum is shown in Fig. 17. Applying a one decay component fit to the data varying the time constant a value of $\tau_\mu = 2.126 \pm 0.013$ μs is obtained which is

significantly lower than the measured value of $\tau_\mu = 2.19703 \pm 0.00004$ μs for the free decay. This indicates clearly the non-negligible influence of muon capture in the stopping material. The solid line in Fig. 17 is the result of a fit superposing μ^+ and μ^- decays with fixed decay constants given above and varying the ratio of the two components [5] resulting in a value of

$\mu^+ / \mu^- = 1.44 \pm 0.39$ for $E_\mu \approx 0.5$ GeV

The quality of the fit expressed in the value of χ^2 per degree of freedom is equivalent to the one component fit.

Although the result is statistically not sufficiently significant it demonstrates the general applicability of the method to the problem of the atmospheric muon charge ratio. Capture reactions with heavier nuclei in the scintillator material and other processes which cannot be separated [5] may have contributed to the unsatisfactory result. Nevertheless, the measured value is of interest since only a few measurements for a threshold of 0.5 GeV exist which are partly contradicting. A dedicated improvement of the measuring device demonstrates the full capability of the method [16].

5. Operation within the KASCADE experiment

5.1 Set-up in the KASCADE experiment

A main part of the KASCADE experiment is a 20 x 16 x 4 m^3 Central Detector (Fig. 18) including as main component an iron-sampling calorimeter for the measurements of the hadronic part of EAS created by high-energetic cosmic rays [2]. The arrangement of the MWPCs in the basement of the detector building was chosen to cover as much as possible the calorimeter area with the potential of a reasonable tracking of penetrating muons. For this purpose the MWPCs are arranged in two layers of 16 chambers each in parallel with the calorimeter layers and with a close covering in the centre of the basement (Fig. 19). The distance between the gas volumes of the layers is 38 cm for all stacks. The absorber (in total 5 cm lead, 172 cm steel and 77 cm concrete) of the calorimeter leads to a threshold for vertical muons of 2.4 GeV , and no muon below 2 GeV can reach the chambers if it is not too inclined to enter the ≈ 4 m high calorimeter from the side. Due to scattering in the absorber muons with energies close to the threshold ($E_\mu < 5$ GeV) have a mean deflection angle of about 1.5 deg. (for vertical incidence) and at higher energies the mean deflection is reduced to 0.5 deg..

The aim of the chamber set-up is the measurement of high energy muons in EAS crossing the calorimeter and correlation measurements of the hadronic and muonic component in air showers. The chambers are triggered by a layer of 456 scintillation detectors mounted in the third gap of the absorber of the calorimeter below 5 cm lead and 36 cm iron ($E_\mu > 400$ MeV). The trigger conditions are either a multiplicity trigger of at least 8 fired scintillators (muon trigger) or one firing detector with a large energy deposit (hadron trigger). The chambers are

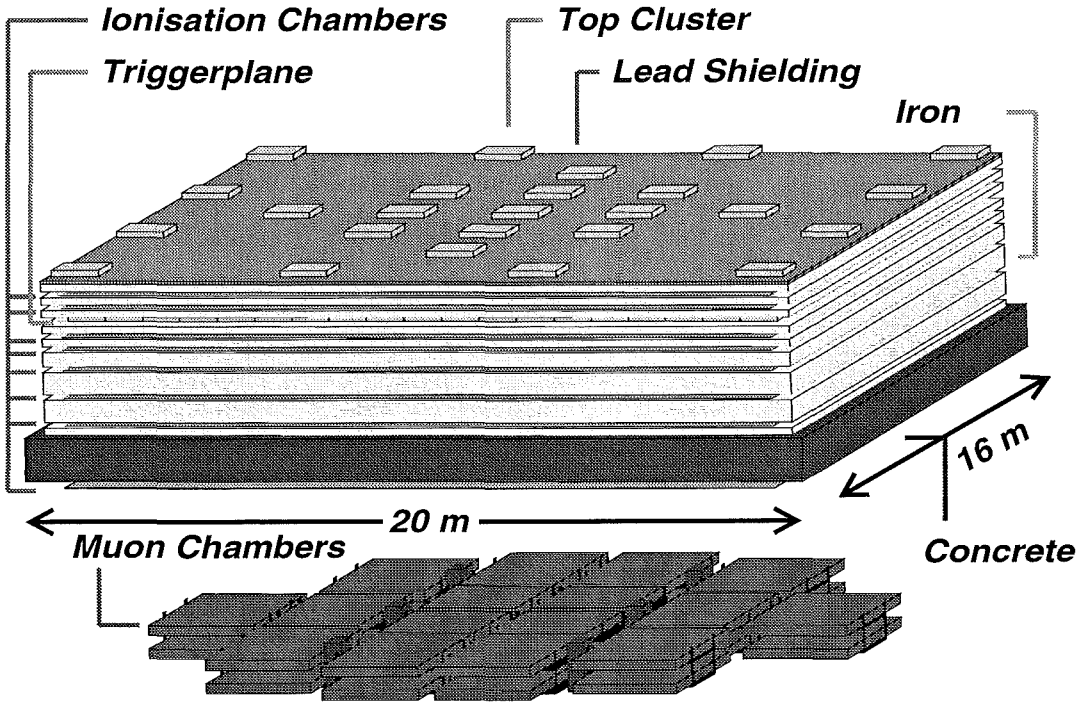

Fig. 18: *Sketch of the KASCADE central detector*

optimised in their operation parameters as described above and the efficiency is monitored parallel to the data acquisition and the parameters for each run are recorded, accordingly. The mean efficiency of the chambers is about 98% and remains constant over long acquisition periods (see Fig. 20).

5.2 Reconstruction procedures

The reconstruction procedure of muons in the MWPC set-up can be divided into different levels, where the first level, the reconstruction of hits in each single chamber, is almost similar to the procedures in the prototype device (see sect. 2.4).

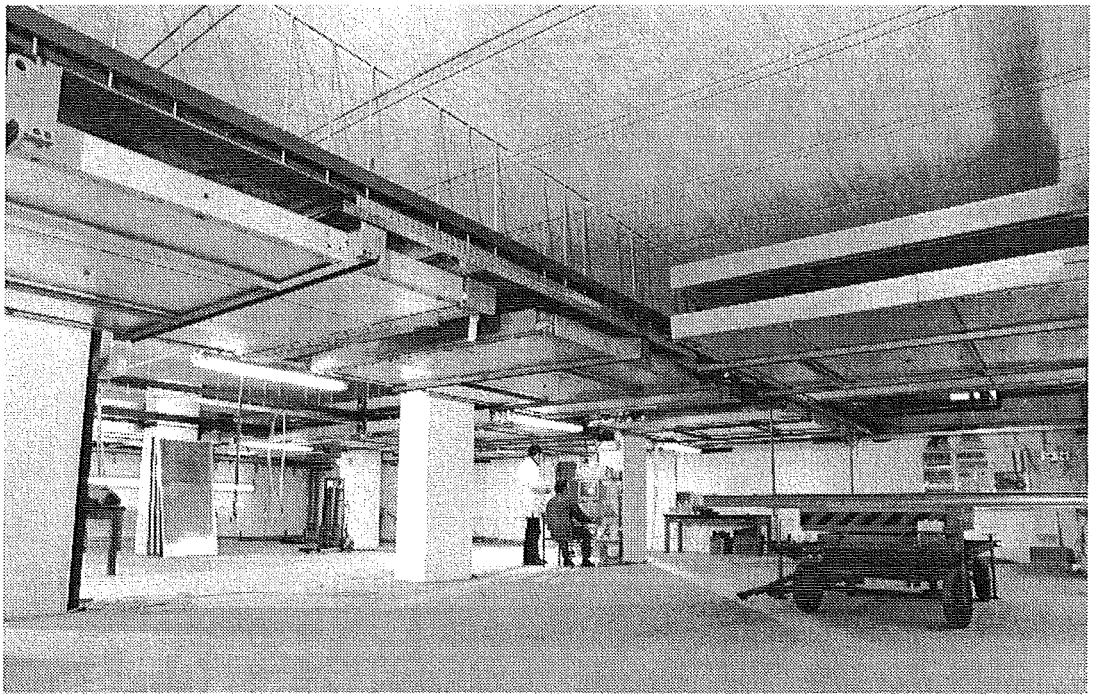

Fig. 19: *View of the MWPCs mounted in the basement of the KASCADE central detector.*

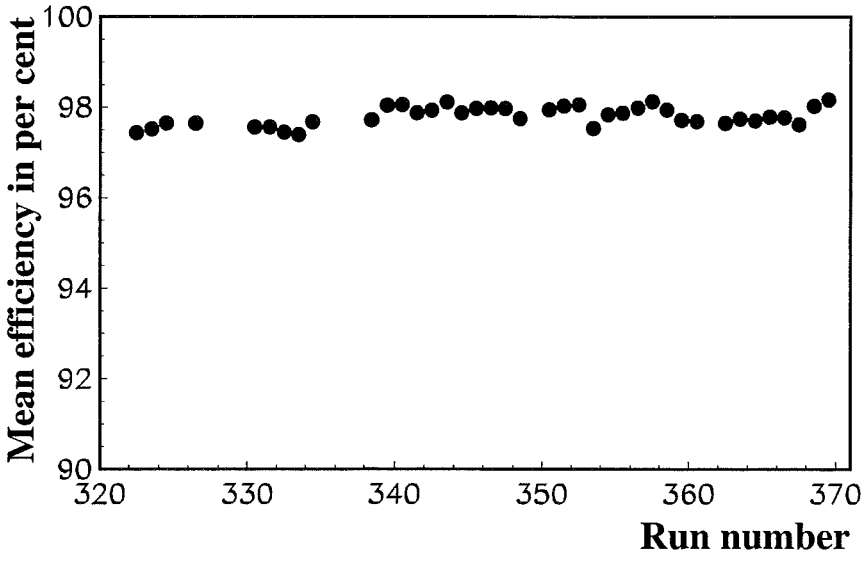

Fig. 20: *Long time efficiency of the chambers in the KASCADE experiment. One run corresponds to an acquisition period of about 2 days.*

For the following steps general information of the event obtained by the analysis of the array detectors of the KASCADE experiment are available, like the coordinates of the centre of the shower, the shower direction, the so-called shower size (i.e. total number of electrons N_e or

charged particles), and the total (N_μ) or reasonably truncated (N_μ^{tr}) number of muons in the shower [17].

Muon tracks in the MWPC are reconstructed from pairs of hits in the two chambers of a stack. Accepted tracks are required to be in reasonable agreement with the shower direction, determined from the array. Thereby, ambiguous hits are efficiently resolved. The spatial resolution of single tracks are $\sigma_x = 0.8$ cm in x-direction (parallel to the anode wires) and $\sigma_y =$ 1.3 cm in y-direction (perpendicular to the anode wires).

Due to the relatively homogeneous distribution of muons in EAS, it is possible to include a procedure for a reduction of misinterpretations due to high-energy δ-electrons in the reconstruction algorithms. From two tracks with a position distance of less than 1 m and with an intersection of the tracks in the absorber material above the chambers one is removed (the one with the larger deviation to the shower direction).

If the multiplicity of fired anodes and cathode strips in an area of $1m^2$ of the chambers is too large for separating hits a so called cluster is reconstructed. The position of such a cluster is defined as the intersection of the centres of gravity of the fired wires and strips. Also for corresponding clusters tracks (hadrons) are reconstructed. However, more than 99% of all triggered events have a muon density below $1/m^2$ where ambiguity effects or hadronic punch-through are negligible.

A typical low density event is shown in Fig. 21 taken from the on-line event display of the data acquisition computer. In the upper part the fired anode wires and cathode strips of all chambers is shown, where pairs of subsequent chambers are mounted one upon the other. In the lower part the same event is shown as reconstructed hits in the trigger plane (dots) and in the MWPCs (stars) clearly indicating the parallel slightly inclined muon tracks. Trigger signals without correlating muon tracks are corresponding to muons with energies between the two thresholds (0.5 - 2.4 GeV) or muons which did not hit the sensitive layer area.

5.3 Muon lateral distributions

The lateral density distribution of muons in extensive air shower measurements is an effective parameter for the reconstruction of the energy spectrum and for the estimation of the chemical composition of the primary cosmic rays [17,18].

Measurements of these lateral distributions of muons with energies larger than 2 GeV are the primary scope of the MWPC set-up at KASCADE. For the determination of the integral lateral distribution (an example see Fig. 22) of the muon density the plane perpendicular to the shower axis is divided into circular areas centred around the shower axis with a width of

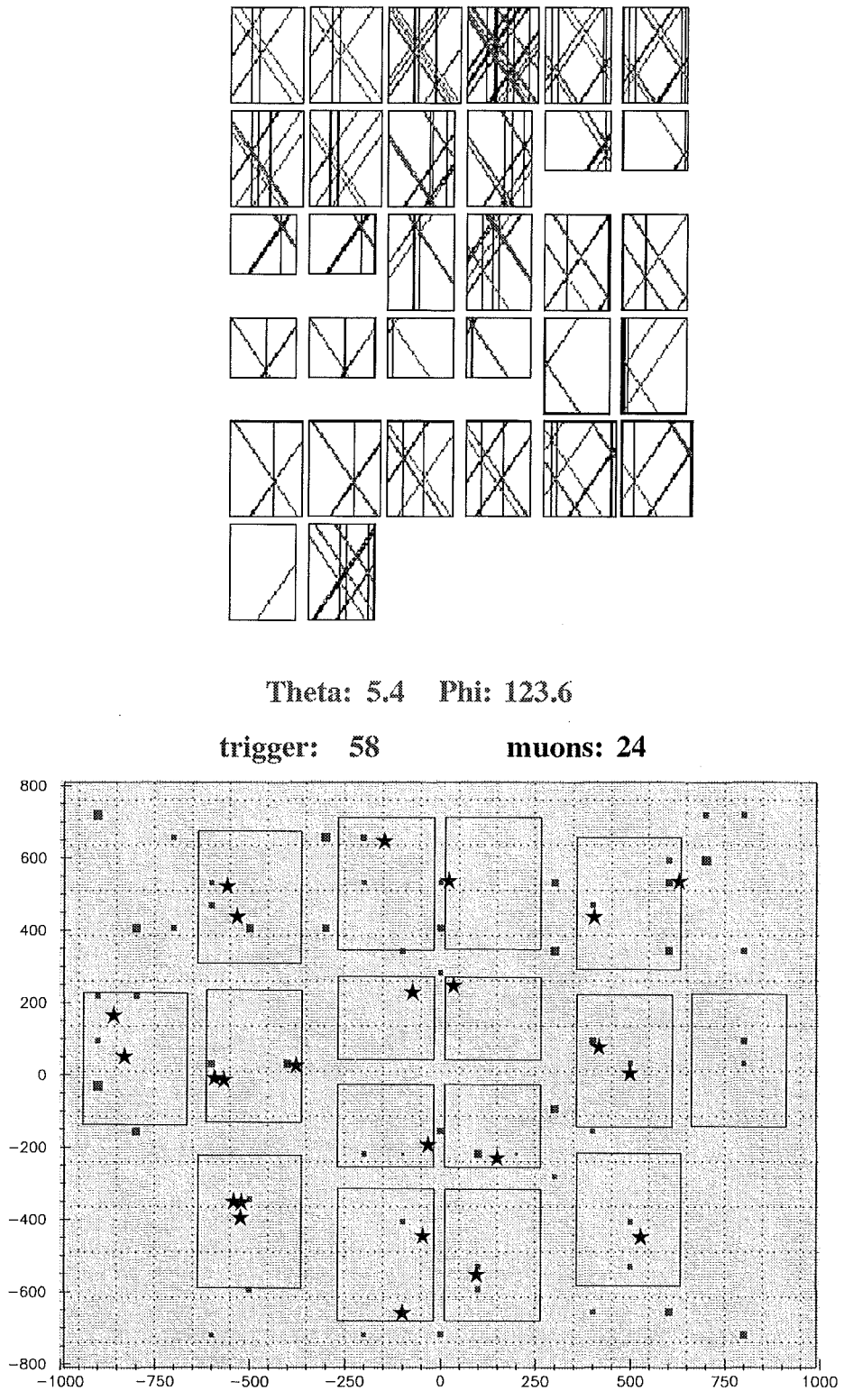

Fig. 21: *Typical low density multi-muon event. Upper part: firing wires and strips of the MWPCs; lower part: reconstructed hits in the MWPCs and trigger layer.*

R=2 m. The lateral distribution is then calculated by summing up the number of muons inside the ring and taking into account the sensitive area. This has been done with a classification of the registered EAS by certain ranges of the values of N_e, N_μ^{tr} and arrival direction. In order to reduce systematic errors in calculating efficiencies no tracks with hits near the edges of any chamber are used in this analysis. In inclined showers, muons entering at the sides of the building would have a lower than nominal energy threshold. In order to achieve uniform thresholds only those areas are used where muons parallel to the shower directions have to penetrate the whole calorimeter. In Fig. 22 lateral distributions are shown for EAS of a large range of the shower size N_e ($\sim 5 \cdot 10^{14} - 3 \cdot 10^{16}$ eV primary energy). The total data acquisition time for the presented statistical accuracy is about 200 days.

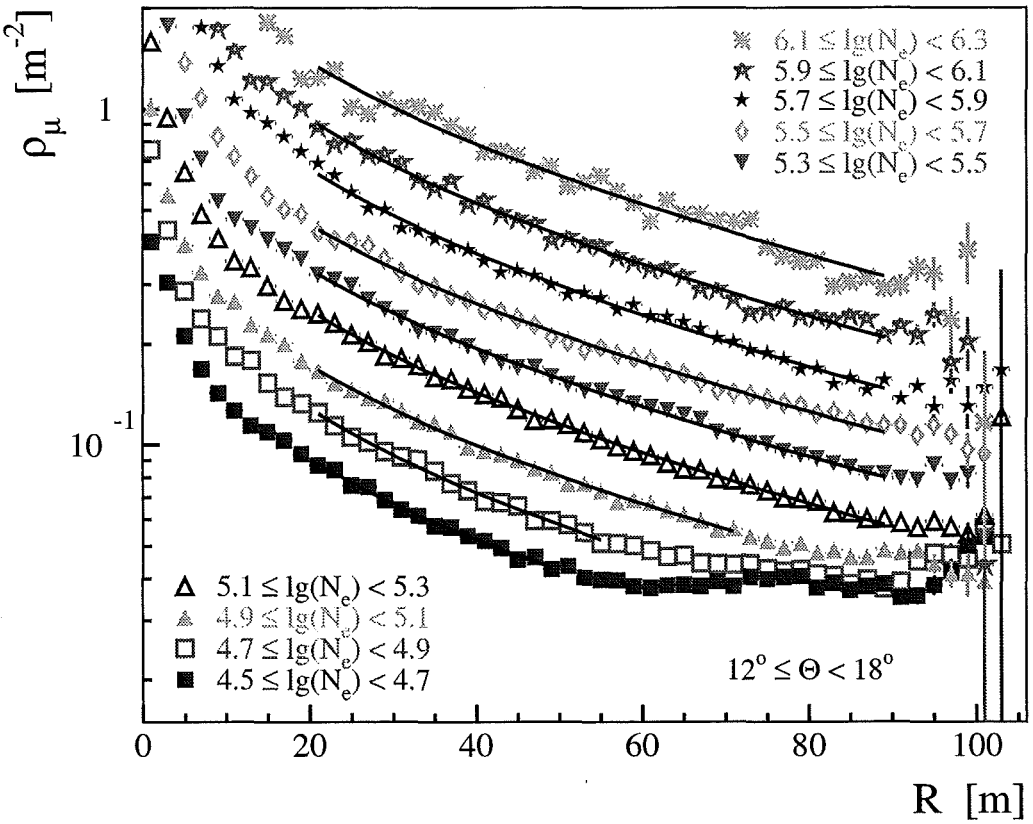

Fig. 22: *Lateral density distributions of muons in extensive air showers measured with the MWPC set-up [17]*

The lines in Fig. 22 represent the range where the measured density is undisturbed by punch-through of the hadronic EAS component (faking muon tracks, ambiguities, loosing muons by

hadronic clusters in the MWPC) at low core distances and by missing triggers at densities below $\rho_\mu = 0.04$ m^2.These ranges are used for detailed studies of the shower development of the muon component at KASCADE [17]. Outside these ranges (especially at small distances, i.e. for central showers) the MWPC system also provides information exceeding the pure number of reconstructed muons

5.4 Central showers

If a high-energy extensive air shower hits the KASCADE central detector with its core a huge number of particles is registered by the different detector components. The hadronic part of such an event is penetrating enough to give signals even below the whole absorber of the calorimeter. Therefore, not only muons are registered in the chambers but also a lot of hits or clusters of hits (Fig. 23) from other origins.

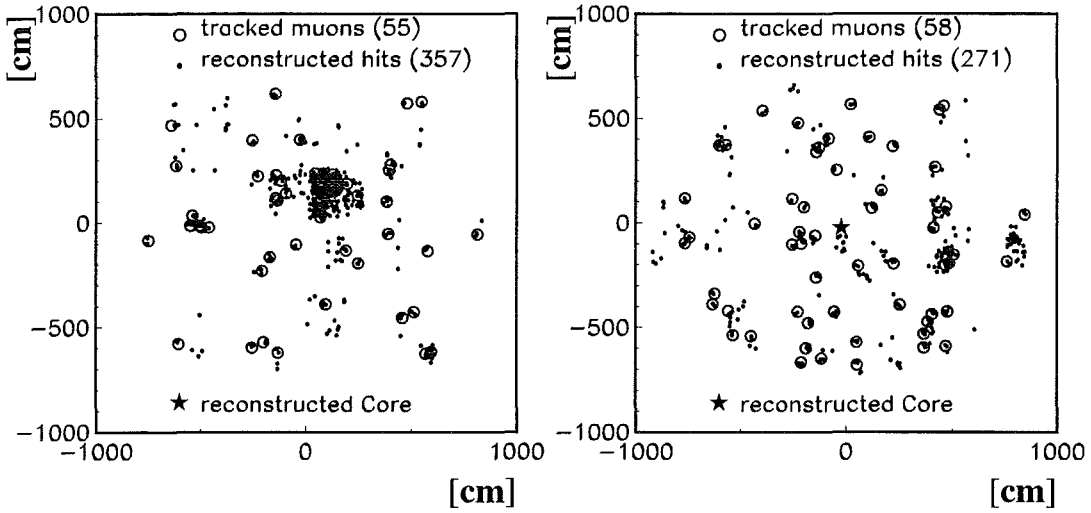

Fig. 23: *Examples for the reconstruction of hits and muon tracks in the MWPC set-up for central high energy showers. The hit distribution is derived from the projected reconstruction crossing points of both chamber planes.*

Dominantly, hits and clusters of different size may be created by:

- muons passing the shielding without any interaction.
- δ-electrons created at the lower end of the shielding (seen mostly with the muon as a pair of two neighboured hits).
- small clusters produced by electromagnetic showers induced by pair production of the muons or by conversion of photons from muon bremsstrahlung or by cascading of δ-electrons.

- clusters of electromagnetic particles from surviving secondaries of hadronic showers stopped in the calorimeter (neutrons).
- large clusters from secondaries of hadrons with energies larger than being absorbed by the calorimeter *(E > 10 TeV)*.
- rare large clusters produced by nuclear interaction of muons with matter. With increasing muon energy the abundance of such interactions is increasing.

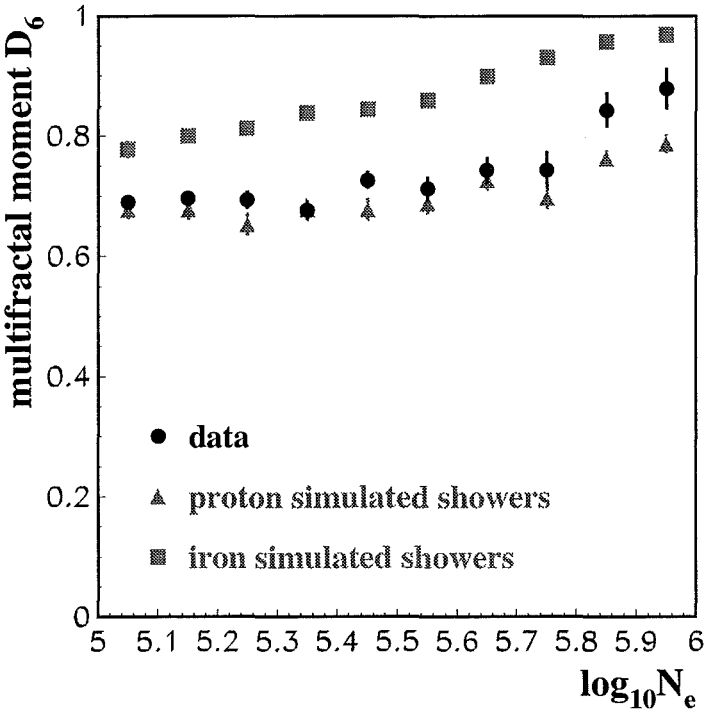

Fig. 24: *The mean of the multifractal parameter D_6 of hit distributions measured by the MWPCs as sensitive parameter for the mass of the primary inducing the air showers.*

Beside the number of the tracked muons the structure of the measured hit distribution for each single event is a relevant parameter for the study of the origin of the air shower generating particle due to the good spatial resolution of the single MWPC. A detailed simulation study has shown [19] that this hit distribution analysed in terms of multifractal moments [20] has the ability to distinguish between different primary masses, at least in combination with further shower parameters like the shower sizes. Figure 24 shows the mass sensitivity of the multifractal parameter D_6 by comparing measured showers with simulations of different

primaries. This parameter is sensitive to the structure of the distribution which is different for different primary masses due to the different development of the shower in the atmosphere, even if other measurable parameters like the shower size or muon numbers are similar. As closer to one as more uniform is the distribution as expected for iron primary generated showers due to their earlier development in the atmosphere and due to the fact that they can approximately be considered as 56 independent sub-showers averaging over statistical fluctuations. These measurements show the possibility of a new successful analysis method on data of large area multiwire proportional chambers. Multiparameter analyses enable a combination of the multifractal parameters with further observables of KASCADE detector systems for a sophisticated reconstruction of the primaries mass and energy on an event-by-event basis [21].

6. Summary and conclusions

A detector system for studies of directional and time correlations for cosmic ray muons was developed. Combining multiwire proportional chambers with scintillation detectors the system detects simultaneously tracks and relative arrival time in multiple muon events.

For the MWPCs taken over from the CELLO-experiment a completely new computer controlled electronics and read-out system has been developed. Adjustment routines for the operational parameters based on the information of single detector components have been used for the set-up. Comparative measurements with argon-isobutane (2:1) and argon-methane (9:1) mixtures demonstrated the capability of the cheaper and easier to handle mixture argon-methane as detector gas. In the purely digital read-out regime high gas amplification could be achieved. The efficiency of the detectors is close to 100% and homogeneous for different zenith angles. Within a time window of 600 ns the efficiency remains constant.

The capability for muon tracking was demonstrated in the prototype arrangement as well as within the KASCADE-experiment where high efficiency and good spatial resolution was achieved even with an arrangement of only two layers of chambers one upon each other. Lateral density distributions and local density structures are measured with the latter arrangement. These informations provide a previously not used handle on the identification of the primary cosmic particle.

Acknowledgements

We would like to thank the Saclay CELLO group and the DESY laboratory for providing us with the MWPCs free of charge. We also thank J. Engler and the late H. Keim who organised the transfer and gave us valuable advice in handling the chambers. The engaged help of the engineering and technical staff of the KASCADE collaboration in reconditioning and mounting the chambers is gratefully acknowledged. This work is embedded in the frame of scientific-technical cooperation projects (WTZ) between Germany and Romania (No. RUM-014-97) .

References

[1] P. Doll et al., (KASCADE Collaboration), The Karlsruhe cosmic ray project KASCADE, Report **KfK-4686,** Kernforschungszentrum Karlsruhe (1990)
H.O. Klages et al., (KASCADE Collaboration), Nucl. Phys. B, Proc. Suppl. **52B** (1997) 92

[2] J. Engler et al., Nucl. Instr. Meth. **A 427** (1999) 528

[3] R. Aleksan et al., Nucl. Instr. Meth. **185** (1981) 95

[4] H.J. Mathes, Report **KfK 5173,** Kernforschungszentrum Karlsruhe 1993

[5] J. Wentz, Report **FZKA 5500**, Forschungszentrum Karlsruhe 1995

[6] F. Herm, Report **KfK 5258B,** Kernforschungszentrum Karlsruhe 1994;
F. Herm et al., Rom. Jour. Phys. **38** (1993) 475

[7] *The I^2C bus specification*, Version 2.1, Philips Semiconductors, Eindhoven 2000

[8] H. Schieler et al., *The Data Acquisition System of the KASCADE Experiment,* Intern. Conf . on Computing in High Energy Physics (CHEP) Berlin (1997), contr. B213

[9] S. Zagromski, H. Bozdog, M. Petcu, Internal Report (unpublished), Forschungszentrum Karlsruhe (1996)

[10] M. Kretschmer, Report **KfK 5295,** Kernforschungszentrum Karlsruhe 1994

[11] D.P. Bhattacharyya, Nouvo Cimento **B 24**(1974) 78

[12] D.P. Bhattacharyya, Phys. Rev. **D 13** (1976) 566

[13] J. Hörandel, Report **KfK 5320,** Kernforschungszentrum Karlsruhe 1994

[14] W. Grandegger, Report **KfK 5122,** Kernforschungszentrum Karlsruhe 1993

[15] T. Suzuki, D.F. Measday, J.P. Roalsvig, Phys. Rev. **C35** (1987) 2212

[16] B. Vulpescu et al., Nucl. Instr. Meth. **A 414** (1998) 205

[17] T. Antoni et al., (KASCADE Collaboration), Astro Part. Phys.**14** (2001) 245

[18] P.R. Blake, W.F. Nash, J.Phys. G: Nucl. Part. Phys. **21** (1995) 129

[19] A. Haungs et al., Nucl. Instr. Meth. **A 372** (1996) 515

[20] A. Aharony, Physica **A 168** (1990) 479

[21] T. Antoni et al., (KASCADE Collaboration), A *Non-Parametric Approach to Infer the Energy Spectrum and the Mass Composition of Cosmic Rays* (to be published)